AMERICAN SOCIETY FOR MICROBIOLOGY | Infection and Immunity®

HOST RESPONSE AND INFLAMMATION

Toll-Like Receptors 2 and 4 Modulate Pulmonary Inflammation and Host Factors Mediated by Outer Membrane Vesicles Derived from *Acinetobacter baumannii*

Chad R. Marion,[a]* Jaewook Lee,[b] Lokesh Sharma,[a] Kyong-Su Park,[b] Changjin Lee,[b] Wei Liu,[a] Pei Liu,[a] Jingjing Feng,[a] Yong Song Gho,[b] Charles S. Dela Cruz[a]

[a]Section of Pulmonary, Critical Care and Sleep Medicine, Yale University School of Medicine, New Haven, Connecticut, USA
[b]Department of Life Sciences, Pohang University of Science and Technology, Pohang, Republic of Korea

ABSTRACT Pneumonia due to Gram-negative bacteria is associated with high mortality. *Acinetobacter baumannii* is a Gram-negative bacterium that is associated with hospital-acquired and ventilator-associated pneumonia. Bacteria have been described to release outer membrane vesicles (OMVs) that are capable of mediating systemic inflammation. The mechanism by which *A. baumannii* OMVs mediate inflammation is not fully defined. We sought to investigate the roles that Toll-like receptors (TLRs) play in *A. baumannii* OMV-mediated pulmonary inflammation. We isolated OMVs from *A. baumannii* cultures and intranasally introduced the OMVs into mice. Intranasal introduction of *A. baumannii* OMVs mediated pulmonary inflammation, which is associated with neutrophil recruitment and weight loss. In addition, *A. baumannii* OMVs increased the release of several chemokines and cytokines in the mouse lungs. The proinflammatory responses were partially inhibited in TLR2- and TLR4-deficient mice compared to those of wild-type mice. This study highlights the important roles of TLRs in *A. baumannii* OMV-induced pulmonary inflammation *in vivo*.

KEYWORDS *Acinetobacter*, TLR, exosomes, lung inflammation

Pneumonia caused by Gram-negative bacteria is a common etiology for admission to the medical intensive care unit and is associated with life-threatening complications, such as sepsis and acute respiratory distress syndrome (1, 2). Severe pneumonia caused by Gram-negative bacteria is also associated with hospital-acquired and ventilator-associated pneumonia and correlates with increased morbidity and mortality (1, 3). *Acinetobacter baumannii* is a Gram-negative bacterium that frequently colonizes hospitalized patients, has many strains that are multidrug resistant, and is associated with high mortality, especially in immunocompromised patients (1, 4–6).

Gram-negative bacteria, including *A. baumannii*, express several virulence factors and toxins, such as lipopolysaccharide (LPS), that are known as pattern-associated molecular patterns (PAMPs) (7, 8). PAMPs are recognized by pattern recognition receptors (PRRs) that are expressed by host cells and function as alert systems for the immune system (8). Toll-like receptors (TLRs) are well-described PPRs that, upon activation, induce the expression of proinflammatory cytokines and recruit immune cells to the site of infection (9, 10). Many TLRs signal through the adaptor protein MyD88 to exert their effects on cytokine expression (11). TLR4, a canonical TLR, recognizes and binds LPS to induce inflammatory cytokine expression and subsequent neutrophil recruitment (9, 10). However, TLR2 also plays an important role in inflammation induced by Gram-negative pathogens. TLR2 can recognize numerous microbial structures, including porins and lipoproteins expressed by *A. baumannii* (9). TLR2 has been shown to be

Citation Marion CR, Lee J, Sharma L, Park K-S, Lee C, Liu W, Liu P, Feng J, Gho YS, Dela Cruz CS. 2019. Toll-like receptors 2 and 4 modulate pulmonary inflammation and host factors mediated by outer membrane vesicles derived from *Acinetobacter baumannii*. Infect Immun 87:e00243-19. https://doi.org/10.1128/IAI.00243-19.

Editor Vincent B. Young, University of Michigan-Ann Arbor

Address correspondence to Yong Song Gho, ysgho@postech.ac.kr, or Charles S. Dela Cruz, charles.delacruz@yale.edu.

* Present address: Chad R. Marion, Section on Pulmonary, Critical Care, Allergy & Immunologic Diseases, Wake Forest School of Medicine, Medical Center Boulevard, Winston-Salem, North Carolina, USA.

C.R.M. and J.L. contributed equally to this work.

Received 3 April 2019
Accepted 11 June 2019
Accepted manuscript posted online 1 July 2019
Published 21 August 2019

important in controlling innate responses while TLR4 was important in clearing bacteria from the lung in the mouse model of *A. baumannii* infection (12). Both TLR2 and TLR4 were reported to be important in the induction of interleukin-8 (IL-8) from airway epithelial cells in response to *A. baumannii* infection (13), while TLR4 was important for inducing signaling in a human monocytic cell line to *A. baumannii*-derived LPS (14).

Alveolar macrophages express TLRs and are among the first cells to sense and respond to foreign materials that enter the lungs, including pathogens (15, 16). Alveolar macrophages have important roles in regulating the recruitment of neutrophils to the lungs by recognizing and binding PAMPs (16, 17). The recruitment of neutrophils to the airways depends on the expression of several TLR-associated cytokines, such as IL-6 and tumor necrosis factor alpha (TNF-α), and the robust recruitment or activation of neutrophils can sometimes damage host tissues by activating inflammasomes, represented as the production of mature forms of IL-1β (18–20).

Bacteria can mediate inflammation both locally and distantly via the release of outer membrane vesicles (OMVs), as reviewed in reference 21. Bacterial OMVs can mediate systemic inflammation in mouse models and may contribute to the development of critical illness in humans during infection (22). *A. baumannii* releases OMVs, but the mechanisms by which the OMVs mediate inflammation in the lungs are not known. We hypothesized that *A. baumannii* generates OMVs that can mediate robust inflammatory responses in TLR-dependent manners. We employed a mouse model to investigate the roles of TLR activation in OMV-mediated inflammation. Here, we sought to characterize the inflammatory response mediated by *A. baumannii* OMVs and study the mechanisms by which *A. baumannii* OMVs mediate proinflammatory cytokine production by employing various TLR-deficient and MyD88-deficient mouse models.

RESULTS

***A. baumannii* releases OMVs.** OMVs were isolated from conditioned medium from *A. baumannii* by differential centrifugation, ultracentrifugation, and iodixanol density gradient ultracentrifugation. Using a three-step (10, 40, and 50%) iodixanol density gradient ultracentrifugation, *A. baumannii* OMVs were settled at fraction 3 (F3), and approximately 6.9 μg of *A. baumannii* OMVs was obtained from 1 liter of culture. Transmission electron microscopy revealed that the purified OMVs contained lipid bilayers and were 30 to 100 nm in diameter (Fig. 1A). Dynamic light scattering also showed the size distribution of the purified OMVs, and the size range was in agreement with that revealed by transmission electron microscopy (Fig. 1B).

***A. baumannii* OMVs can be detected in the mouse lungs after intranasal administration.** To determine if *A. baumannii* OMVs can be detected in the lung parenchyma after intranasal administration, we measured the concentrations of *A. baumannii* OMV components in the lung tissue of mice after administering various amounts of *A. baumannii* OMVs. Lung tissues were collected at 6, 12, 24, and 48 h after intranasal administration, and *A. baumannii* OMVs were detected using anti-*A. baumannii* OMV antibody. *A. baumannii* OMVs were detected in a dose-dependent manner (Fig. 1C). The amounts of *A. baumannii* OMV components in the lung tissues at 6, 12, 24, and 48 h after intranasal administration of OMVs (10 μg) were determined (Fig. 1D). *A. baumannii* OMV components were maximally detected at 6 h and then subsided but continued to be detected until 48 h after intranasal administration.

***A. baumannii* OMVs mediate neutrophilic predominant pulmonary inflammation.** After determining that *A. baumannii* OMVs can be detected in the lung parenchyma after OMV administration, we next sought to determine if *A. baumannii* OMVs could mediate pulmonary inflammation. *A. baumannii* OMVs were intranasally administered into mice, and the bronchoalveolar lavage (BAL) fluids were obtained to perform differential cell counts. At all doses of *A. baumannii* OMVs tested, the numbers of total cells and neutrophils were significantly increased in the BAL fluid in a dose-dependent manner (Fig. 2A). Neutrophils were the predominant cell type among the recruited cells in BAL fluid. When *A. baumannii* OMVs (10 μg in total protein amounts) were intrana-

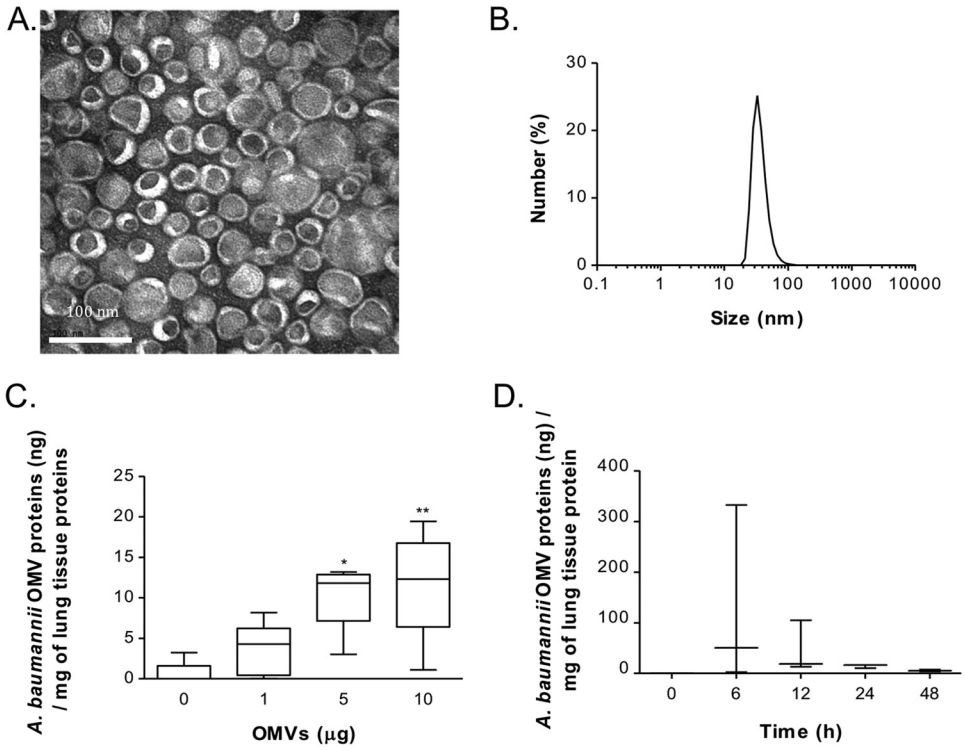

FIG 1 Characterization of *A. baumannii* OMVs and OMV component detection in the lungs. (A) Transmission electron microscopy indicating that the purified OMVs have lipid bilayered structures. (B) Size distribution of the purified OMVs determined by dynamic light scattering, with the diameter ranging from 30 to 100 nm. (C) Various amounts of *A. baumannii* OMVs (0, 1, 5, and 10 μg in total protein amounts) were intranasally introduced into mice, and the amounts of OMV components were measured at 24 h after intranasal instillation of the OMVs. (D) *A. baumannii* OMVs (10 μg) were intranasally introduced to mice, and the amounts of OMV components were measured at 0, 6, 12, 24, and 48 h after intranasal instillation of the OMVs. *, $P < 0.05$; **, $P < 0.01$.

sally administered to mice, *A. baumannii* OMVs mediated pulmonary consolidation up to 48 h after OMV administration (Fig. 2B).

We next sought to determine if the induction of pulmonary inflammation by *A. baumannii* OMVs was associated with weight loss. The ability of mice to maintain their body weights after stimulation with microbes or microbial products is a commonly utilized marker of general health (23, 24). To determine the health of *A. baumannii* OMV-administered mice, we measured the body weight of mice at 24 h after stimulation with *A. baumannii* OMVs (0, 1, 5, and 10 μg in total protein amounts). All mice stimulated with *A. baumannii* OMVs developed body weight loss in a dose-dependent manner (Fig. 2C). However, *A. baumannii* OMV administration did not cause any mortality in the mice up to 24 h with any of the tested doses (Fig. 2D).

***A. baumannii* OMVs mediate the release of proinflammatory chemokines and cytokines.** We next investigated the chemokine and cytokine milieu in the lungs of mice instilled with *A. baumannii* extracellular vesicles (EV), which could promote neutrophilic pulmonary inflammation. Given that the numbers of recruited neutrophils in BAL fluids were not significantly different between 5 and 10 μg of *A. baumannii* OMVs, the concentrations of chemokines CCL2 and CXCL1 as well as cytokines IL-6, TNF-α, gamma interferon (IFN-γ), and IL-1β were measured after intranasal administration of 0, 1, and 5 μg of *A. baumannii* OMVs. At 24 h after intranasal administration of 1 and 5 μg of the OMVs, the concentrations of chemokines and cytokines were significantly increased compared with those of the control (Fig. 3A to F). The concentrations of CCL2, IL-6, and IL-1β were increased in a dose-dependent manner (Fig. 3A, C, and F, respectively), whereas a saturation effect was observed at the 1-μg dose for CXCL1, TNF-α, and IFN-γ (Fig. 3B and D and E, respectively).

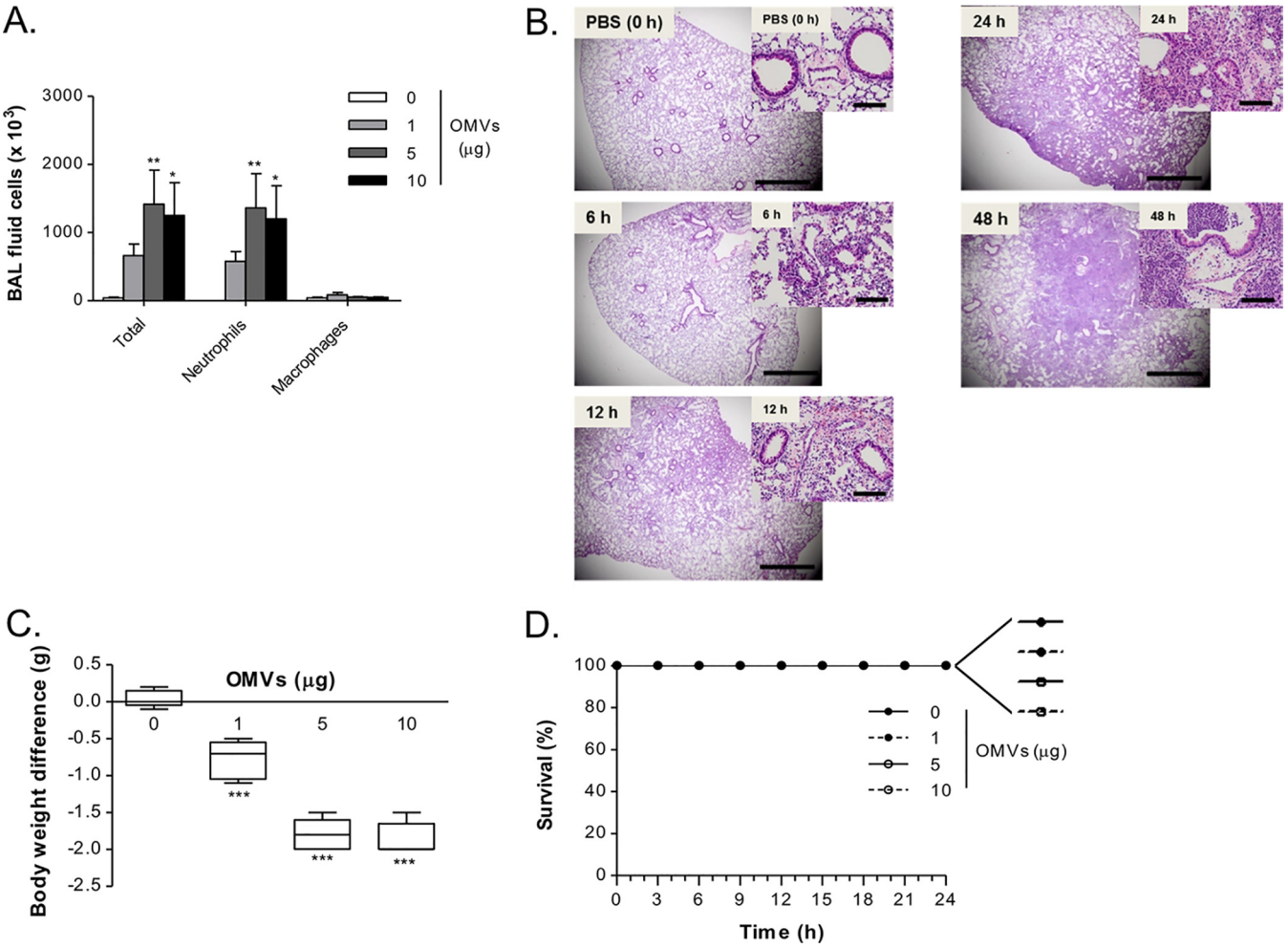

FIG 2 Outer membrane vesicles from *A. baumannii* induce rapid neutrophil recruitment to the lungs. (A) Dose-dependent effects of *A. baumannii* OMVs on the numbers of BAL fluid cells. Various amounts of *A. baumannii* OMVs (0, 1, 5, and 10 μg in total protein amounts) were intranasally introduced to mice, and at 24 h after intranasal instillation of the OMVs, the numbers of BAL fluid total cells, neutrophils, and macrophages were counted. (B) Time course (0, 6, 12, 24, and 48 h) of pulmonary inflammation mediated by *A. baumannii* OMVs. Hematoxylin and eosin staining of the lung sections of mice was conducted at different time points after intranasal instillation of *A. baumannii* OMVs (10 μg). Scale bars, 1 mm (low magnification) and 100 μm (high magnification). (C and D) Dose-dependent effects of *A. baumannii* OMVs on body weight loss and survival. (C) Various amounts of *A. baumannii* OMVs (0, 1, 5, and 10 μg in total protein amounts) were intranasally introduced to mice, and at 24 h after intranasal instillation of the OMVs, the body weight of mice was measured and body weight difference was calculated by comparison to mice which were not instilled with OMVs. (D) Survival of mice was monitored every 3 h for 1 day. *, $P < 0.05$; **, $P < 0.01$; ***, $P < 0.001$.

IL-1β, an inflammasome-associated cytokine, is induced in a two-step process (25, 26). First, pro-IL-1β is expressed after TLR activation. The second signal is the action of inflammasome complex formation via recognition of damage-associated molecular patterns. Inflammasome activation induces caspase-dependent processing of pro-IL-1β to active IL-1β. In our model, IL-1β is expressed in a dose-dependent manner (Fig. 3F). These data suggest that *A. baumannii* OMVs mediated neutrophil recruitment via TLR activation and that *A. baumannii* OMVs were sufficient to mediate the release of damage-associated molecular patterns and trigger inflammasome activation.

Effects of *A. baumannii* OMVs on cytokine release and regulation by TLR2 and TLR4. Macrophages are among the first cells to recognize foreign materials that enter the lungs and play important roles in recruiting neutrophils to the lungs (16, 17). We sought to determine which PRR(s) expressed by macrophages plays an important role in the release of proinflammatory cytokines in response to *A. baumannii* OMVs. RAW264.7 (a mouse macrophage cell line) cells were stimulated with various concentrations of *A. baumannii* OMVs (0, 0.01, 0.1, and 1.0 ng/ml total protein concentrations)

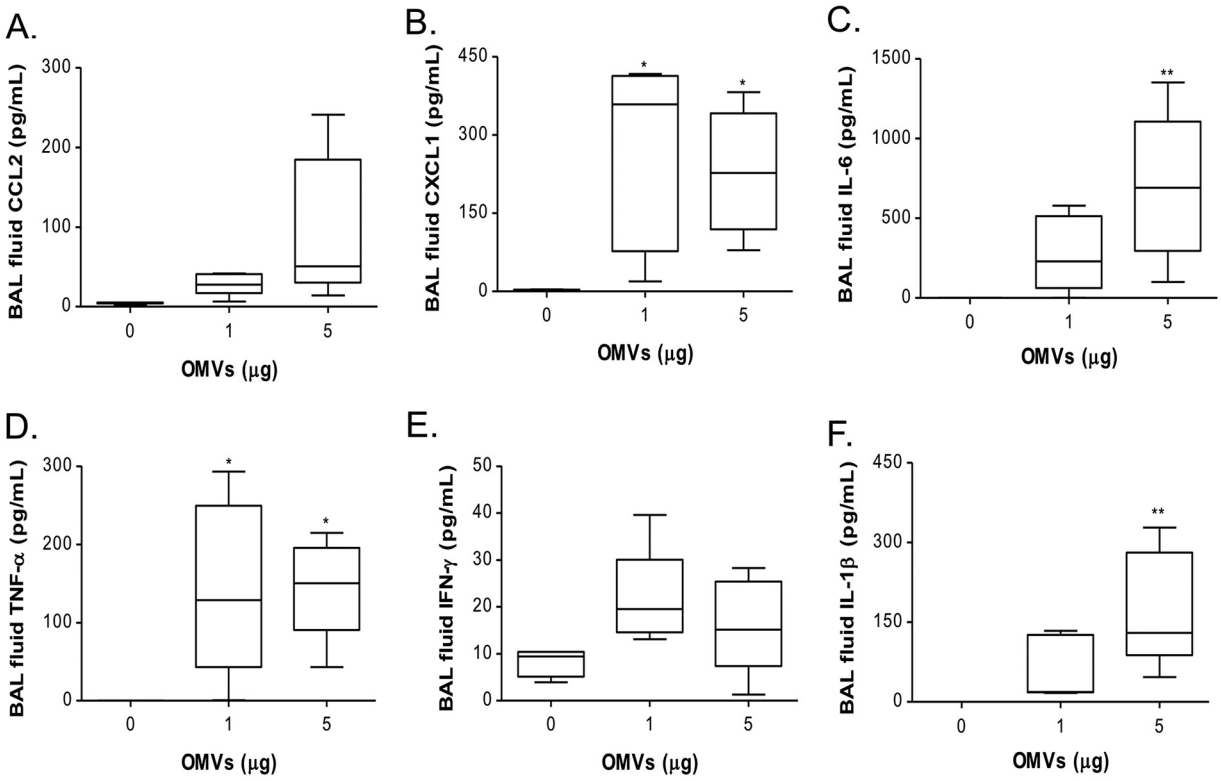

FIG 3 Dose-dependent effects of *A. baumannii* OMVs on the BAL concentrations of chemokines and cytokines. Mice were intranasally introduced to *A. baumannii* OMVs (0, 1, and 5 μg in total protein amounts), and at 24 h after intranasal instillation of the OMVs, the BAL concentrations of chemokines and cytokines were determined. The BAL concentrations of chemokines CCL2 (A) and CXCL1 (B) as well as cytokines IL-6 (C), TNF-α (D), IFN-γ (E), and IL-1β (F) were measured. *, $P < 0.05$; **, $P < 0.01$.

for 12 h. *A. baumannii* OMVs mediated the release of IL-6 and TNF-α in a dose-dependent manner (Fig. 4A and B).

To investigate the roles of TLRs in *A. baumannii* OMV-mediated cytokine release, we employed peritoneal macrophages derived from wild-type mice and mice deficient in TLR2, TLR4, or TLR adaptor protein MyD88. Stimulation of wild-type peritoneal macrophages with *A. baumannii* OMVs again mediated the release of IL-6 in a dose-dependent manner (Fig. 4C). *A. baumannii* OMV-mediated release of IL-6 was significantly decreased in peritoneal macrophages derived from mice deficient in TLR2, TLR4, or MyD88 compared to that from wild-type mice. However, unlike peritoneal macrophages from TLR4- or MyD88-deficient mice, the cytokine responses from TLR2-deficient mice were not completely abrogated in the release of IL-6 in response to stimulation with *A. baumannii* OMVs.

Roles of TLR2 and TLR4 in *A. baumannii* OMV-mediated pulmonary inflammation *in vivo*. We next sought to determine the roles of TLR2 and TLR4 in *A. baumannii* OMV-mediated pulmonary inflammation *in vivo*. *A. baumannii* OMVs (5 μg in total protein amounts) were intranasally administered into wild-type as well as TLR2- and TLR4-deficient mice. Host and inflammatory responses were measured by body weight loss, BAL fluid cell count, lung histology, and cytokine release. Stimulation of mice with *A. baumannii* OMVs mediated body weight loss throughout the time course of stimulation (Fig. 5A). Stimulation of either wild-type or TLR2-deficient mice with *A. baumannii* OMVs mediated similar levels of body weight loss, but there was more significant body weight loss in TLR4-deficient mice.

The numbers of total cells, neutrophils, macrophages, and lymphocytes in the BAL fluids were counted at 6 and 24 h after intranasal administration of *A. baumannii* OMVs (Fig. 5B to D). Higher numbers of total leukocytes, neutrophils, and macrophages were recruited at 24 h after intranasal administration than at 6 h after administration. Higher

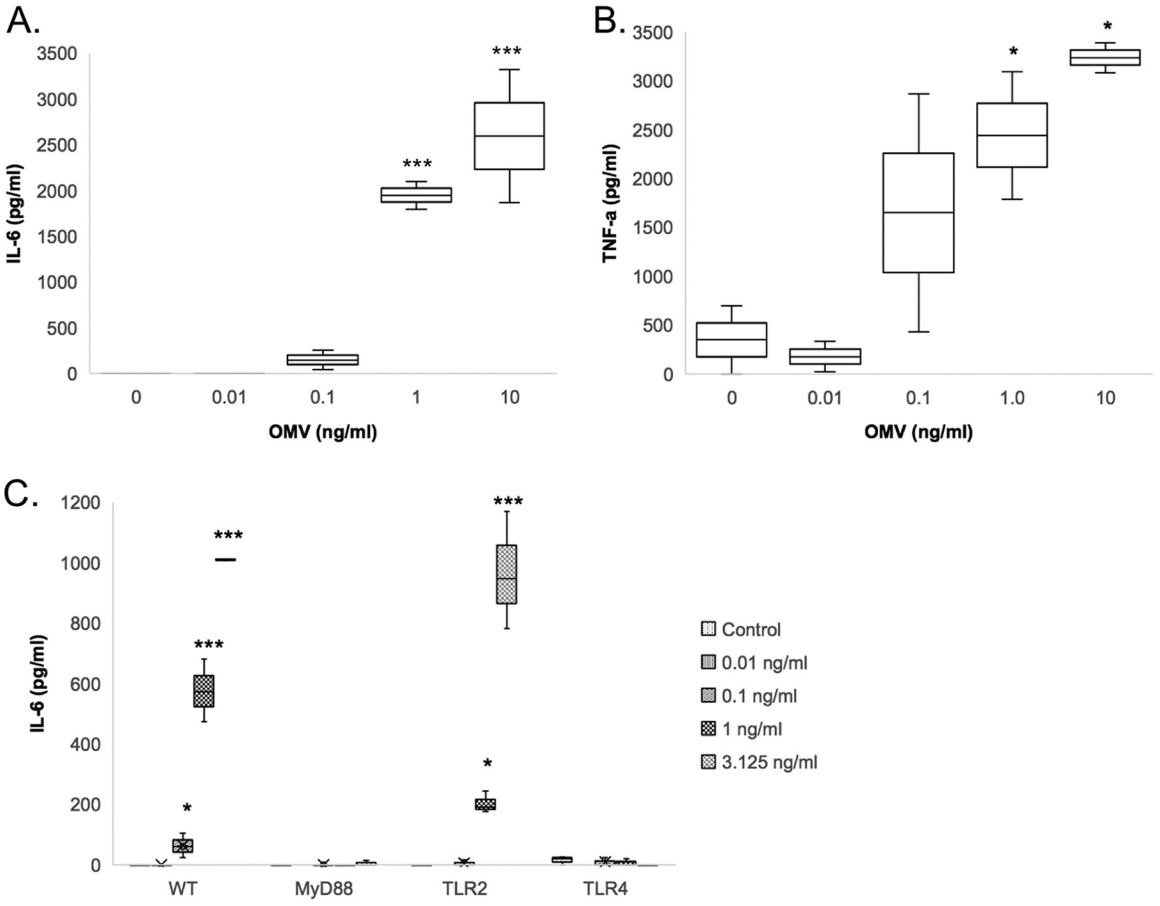

FIG 4 Effects of *A. baumannii* OMVs on cytokine release by macrophages and regulation by TLR2 and TLR4. (A and B) Various concentrations of *A. baumannii* OMVs (0, 0.01, 0.1, and 1 ng/ml in total protein concentrations) were added to RAW264.7 cells (mouse macrophage cell line) *in vitro*, and at 12 h after stimulation with the OMVs, the concentrations of IL-6 (A) and TNF-α (B) in conditioned media were measured. (C) Peritoneal macrophages from wild-type, MyD88 knockout (KO), TLR2 KO, and TLR4 KO mice were stimulated with various concentrations of *A. baumannii* OMVs (0, 0.01, 0.1, and 1 ng/ml in total protein concentrations). At 12 h after stimulation with the OMVs, the concentrations of IL-6 in conditioned media were measured. *, $P < 0.05$; ***, $P < 0.001$.

numbers of total leukocytes and neutrophils were recruited in TLR2-deficient mice than in wild-type mice at 6 h after administration, whereas there were no significant differences between wild-type and TLR4-deficient mice at that time point. However, there were significantly reduced numbers of total leukocytes and neutrophils recruited in TLR4-deficient mice at 24 h after administration, whereas there were no significant differences between wild-type and TLR2-deficient mice at that time point (Fig. 5B and C). Regarding the number of recruited macrophages, there were no significant differences between wild-type and TLR2- as well as TLR4-deficient mice at 6 h after administration. However, at 24 h after administration, fewer numbers of macrophages were recruited in TLR4-deficient mice than in wild-type and TLR2-deficient mice (Fig. 5D). Lung histology of wild-type and TLR2- as well as TLR4-deficient mice stimulated with *A. baumannii* OMVs revealed that there was more severe pulmonary consolidation in wild-type mice than in both TLR2- and TLR4-deficient mice, with TLR4-deficient mice exhibiting much less pulmonary inflammation and consolidation (Fig. 5E and F). However, we saw an increase in weight loss in TLR2 and TLR4 knockout mice (Fig. 5G).

TLR2 and TLR4 mediate proinflammatory cytokine production induced by *A. baumannii* OMVs. The concentrations of cytokines IL-6, TNF-α, and IL-1β in BAL fluids were measured at 6 and 24 h after intranasal administration of *A. baumannii* OMVs (Fig. 6A to F). Compared to that of wild-type mice, the release of IL-6 was increased in TLR2-deficient mice at 6 h after administration, whereas there were no significant

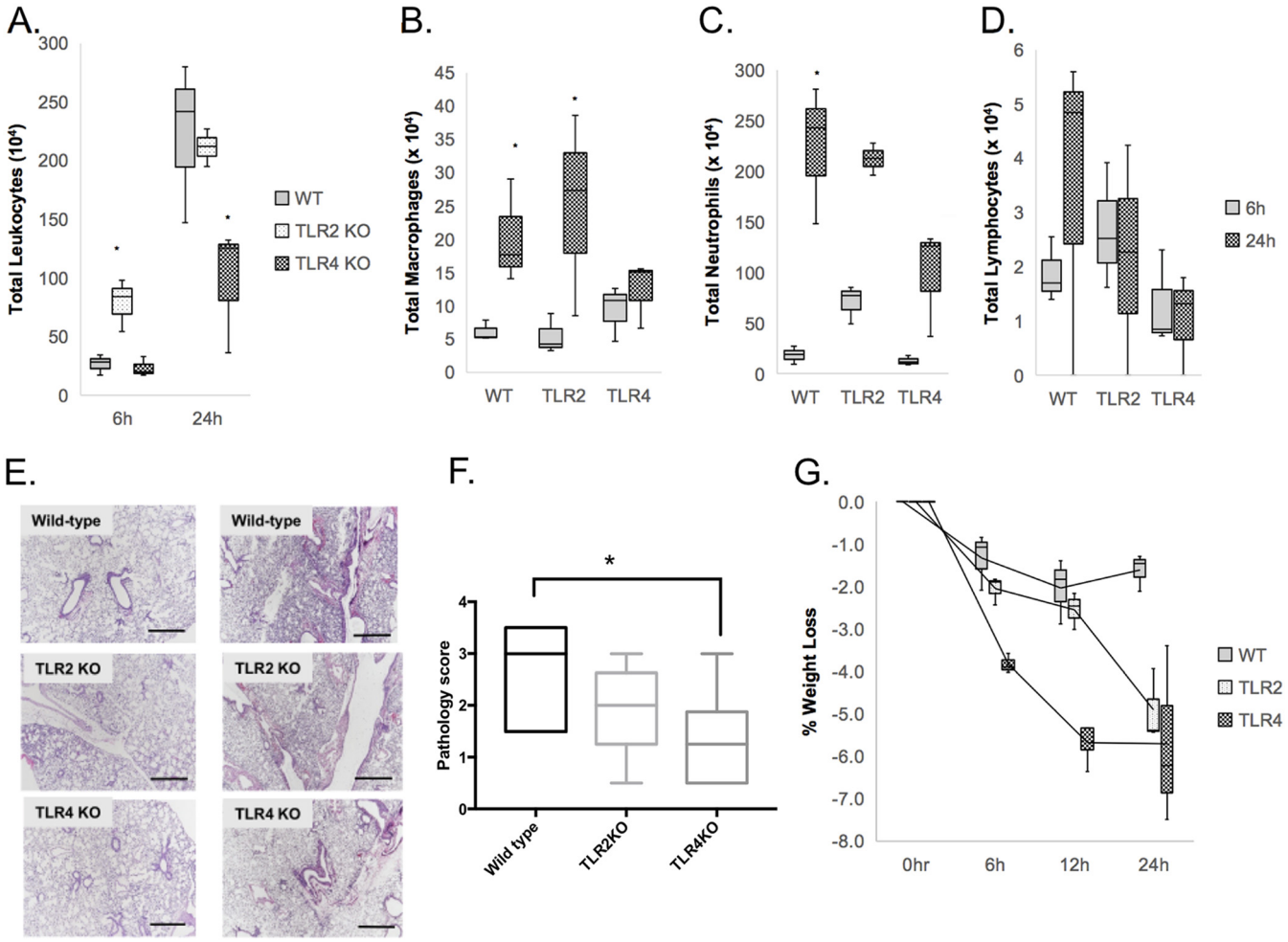

FIG 5 Roles of TLR2 and TLR4 in *A. baumannii* OMV-mediated pulmonary inflammation *in vivo*. *A. baumannii* OMVs (5 μg in total protein amounts) were intranasally introduced to wild-type as well as TLR2- and TLR4-deficient mice. (A to D) At 6 h and 24 h after intranasal instillation of the OMVs, the numbers of BAL fluid total cells (A), macrophages (B), neutrophils (C), and lymphocytes (D) were counted. (E) Hematoxylin and eosin staining of the lung sections of mice was conducted at 6 h and 24 h after intranasal instillation of the OMVs. Scale bars, 100 μm. (F) Pathology score of WT, TLR2 knockout (KO), and TLR4 KO mice treated with OMV at 24 h. (G) Time course (0, 6, 12, and 24 h) of body weight loss of mice. *, $P < 0.05$.

differences between wild-type and TLR4-deficient mice at that time point. However, the release of IL-6 was decreased in both TLR2- and TLR4-deficient mice at 24 h after administration (Fig. 6A). The release of TNF-α was decreased in TLR4-deficient mice at both 6 and 24 h after administration compared to that of wild-type mice, whereas there were no significant differences between wild-type and TLR2-deficient mice at those time points (Fig. 6B). The release of IL-1β was increased at 24 h after administration in wild-type and TLR2-deficient mice compared to that 6 h after administration. However, stimulation of TLR4-deficient mice similarly induced the release of IL-1β at 6 and 24 h after administration. Compared to that of wild-type mice, the release of IL-1β was decreased in both TLR2- and TLR4-deficient mice at 24 h after administration (Fig. 6C).

***A. baumannii* OMVs induce MAPK in the lung.** OMV-treated mouse lungs exhibited increased mitogen-activated protein kinase (MAPK)-related phosphorylated P42/44 (or Erk1/2) compared to that of phosphate-buffered saline (PBS)-treated lungs (Fig. 7A to C), showing increased phosphorylated P42/44 in proportion to total P42/44 or β-actin as a control. Proinflammatory cytokines such as IL-1β, IL-6, and TNF-α were increased in OMV-treated lungs compared to levels in PBS-treated controls, as measured by semiquantitative reverse transcription-PCR (Fig. 7D to F). We were also interested in determining if type I interferons such as IFN-α and IFN-β were modulated with OMV treatment. We found that there were no significant differences between

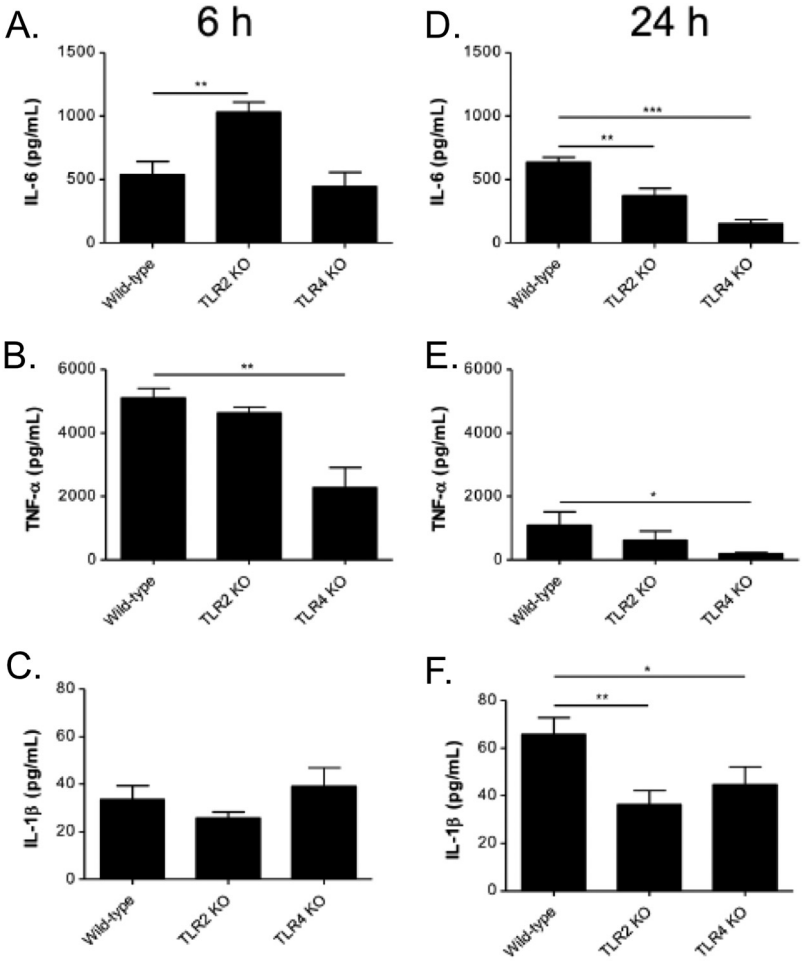

FIG 6 Roles of TLR2 and TLR4 in *A. baumannii* OMV-mediated cytokine release *in vivo*. *A. baumannii* OMVs (5 μg in total protein amounts) were intranasally introduced to wild-type as well as TLR2- and TLR4-deficient mice. At 6 h and 24 h after intranasal instillation of the OMVs, the BAL concentrations of cytokines IL-6 (A and D), TNF-α (B and E), and IL-1β (C and F) were measured. *, $P < 0.05$; **, $P < 0.01$; ***, $P < 0.001$.

PBS-treated and OMV-treated lungs in the induction of IFN-α4 or IFN-β, suggesting that the OMV mediated its effect through a MyD88 pathway and not a TRIF or TRAM pathway. The OMVs induced increased IFN-γ in the lungs compared to that of the PBS control (Fig. 8).

To determine if the proinflammatory effects of *A. baumannii* OMVs were due to LPS, a TLR4 agonist, peritoneal macrophages derived from wild-type mice were treated with PBS, LPS, or *A. baumannii* OMVs with or without polymyxin B (PMB), an inhibitor of LPS stimulation. The release of TNF-α was significantly increased by LPS and *A. baumannii* OMVs compared to that of the control group. PMB almost completely reduced the release of TNF-α from macrophages stimulated with LPS, but it only partially decreased the release of TNF-α from macrophages stimulated with OMVs (see Fig. S1 in the supplemental material), suggesting LPS plays a role in OMV-mediated TNF-α release.

DISCUSSION

Pneumonia caused by *A. baumannii* results in respiratory failure, sepsis, acute respiratory distress syndrome, and high mortality in patients admitted to medical intensive care units (1, 2). Poor clinical outcomes can result from overexuberant inflammatory responses to infectious pathogens, which result in damage to the lungs during pneumonia (27). Understanding the pathogen-host interactions that result in inflammation-mediated damage to host tissues is needed to prevent and treat severe

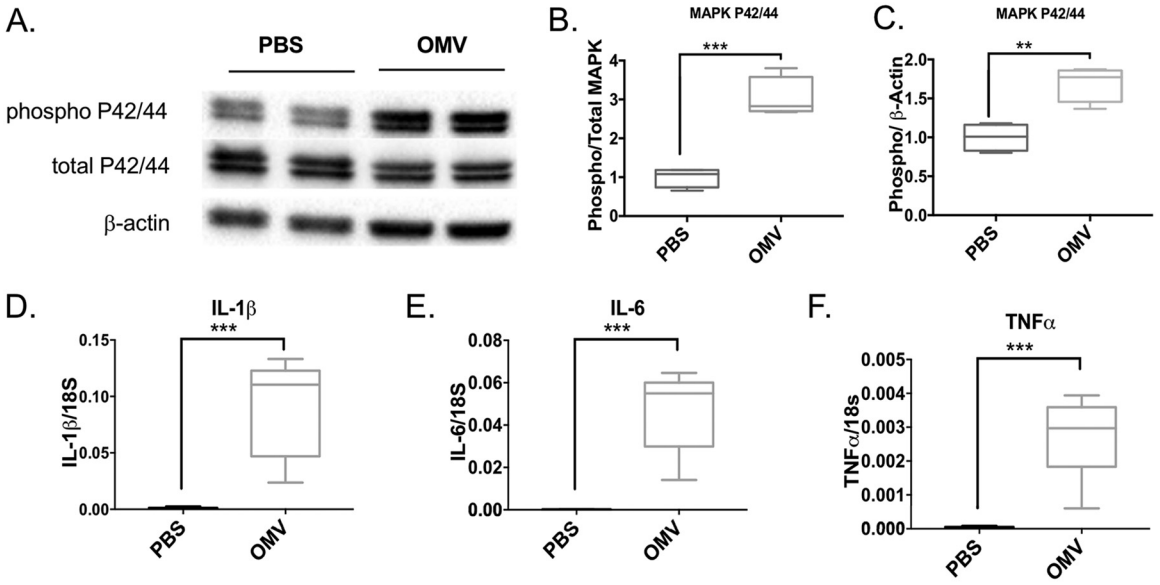

FIG 7 OMVs activate MAPK and NF-κB pathways in the mouse lung. C57BL/6 mice were intranasally administered *A. baumannii* OMVs (5 μg in total protein amounts) or PBS as a control. Mice were sacrificed at 6 h postintranasal administration of OMVs to harvest lung samples. MAPK activation was measured by Western blot analysis of lung samples. (A) A representative Western blot image. (B and C) Densitometry analysis of band intensity was performed. The levels of phospho-MAPK were normalized to total MAPK (B) or β-actin (C). The NF-κB activation was measured by activation of downstream genes in the NF-κB pathway. (D to F) The expression levels of IL-1β (D), IL-6 (E), and TNF-α (F) were measured by qPCR. $P < 0.01$ (**) and $P < 0.005$ (***) compared to the control group. $n = 6$ mice in each group.

complications of pneumonia. Here, we sought to investigate the mechanisms by which *A. baumannii* OMVs, independent of bacterial growth, mediate pulmonary inflammation. Currently, OMVs are thought to play important roles in intercellular communication during acute infections (21, 28, 29). Understanding the role that OMVs play in systemic inflammation can provide insight as to the mechanisms by which acute bacterial infections can induce severe systemic inflammation and death despite adequate antimicrobial administration. We hypothesized that *A. baumannii* OMVs would mediate pulmonary inflammation in TLR-dependent manners because TLRs play roles as first-line detectors of pathogens. To investigate this question, we employed mice with genetic deficiencies in TLRs and the downstream adaptor MyD88 and measured inflammatory responses *in vivo* and *in vitro*. We demonstrated that stimulation with *A. baumannii* OMVs mediated robust recruitment of neutrophils to the lungs in a dose- and time-dependent manner. Neutrophil recruitment into the lungs increased over time and was associated with increased consolidation of the lungs. We discovered that *A. baumannii* OMVs mediated significant weight loss, an important clinical indicator of severity of illness, in a dose-dependent manner.

Neutrophils play central roles in the clearance of infectious organisms during acute infection by *A. baumannii* (30). The active recruitment of neutrophils to the lungs depends on the early identification of infectious pathogens by resident cells of the lung, including alveolar macrophages, and is orchestrated by the expression of multiple proinflammatory cytokines through TLR activation (15–17). Independent of bacterial growth, bacterial OMVs can result in inflammatory responses that may lead to immune dysregulation and death due to sepsis. We sought to define the roles TLR2 and TLR4 play in regulating *A. baumannii* OMV-mediated neutrophil recruitment and release of proinflammatory cytokines.

Both TLR2 and TLR4 are expressed on the cell surface of macrophages and signal via the common adaptor protein MyD88 (11, 20). IL-6 is a proinflammatory cytokine secreted by macrophages that leads to the recruitment of neutrophils to the sites of infection (18, 20). *A. baumannii* OMV-mediated release of IL-6 was significantly decreased in peritoneal macrophages derived from mice deficient in TLR2, TLR4, or MyD88

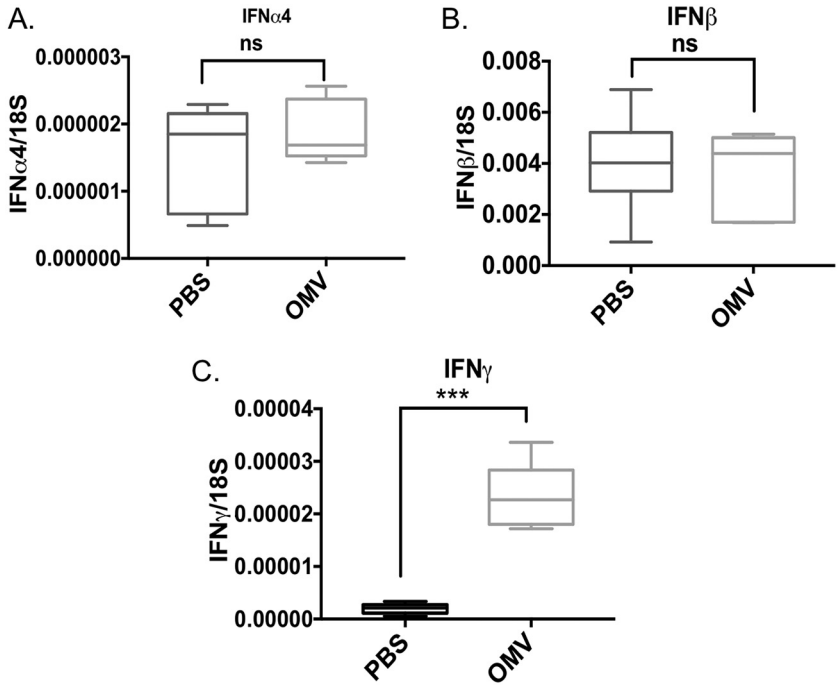

FIG 8 *A. baumannii* OMVs activate interferon gamma in the lung. To understand if OMV contributes to the activation of the interferon pathway, we measured expression of interferon genes in the samples mentioned in Fig. 7 using qPCR. The levels of interferon alpha mRNA (A) and interferon beta mRNA (B) were not different in OMV-treated mice from those in the controls. In contrast, expression of interferon gamma was significantly elevated in the lungs of mice that were intranasally administered with OMVs (C), suggesting specificity of interferon activation by OMVs. ns, not significant; ***, $P < 0.005$. $n = 6$ mice in each group.

compared to those from wild-type mice. However, unlike peritoneal macrophages from TLR4- or MyD88-deficient mice, those from TLR2-deficient mice were not completely abrogated in the release of IL-6 in response to stimulation with *A. baumannii* OMVs. The recruitment of leukocytes, especially neutrophils, is decreased in TLR4-deficient mice compared to that in wild-type mice, whereas the numbers were not decreased in TLR2-deficient mice. The release of proinflammatory cytokines was decreased but not completely abrogated in both TLR2- and TLR4-deficient mice compared to those in wild-type mice. These findings suggest that both TLR2 and TLR4 have roles in recognizing *A. baumannii* OMVs, but TLR4 has a larger role than TLR2 does. Neutrophil recruitment in response to *Pseudomonas aeruginosa* OMVs is at least partially dependent on TLR2 (9). This suggests that *A. baumannii* OMVs express specific bacterial proteins that signal more through TLR4, which is not expressed on *P. aeruginosa* OMVs (22). *A. baumannii* OMVs express numerous bacterial proteins, but the specific ligand responsible for TLR4-mediated neutrophil recruitment and release of proinflammatory cytokines is currently not known (5, 31, 32). *A. baumannii* OMVs being preferentially more reliant on TLR4 for inducing inflammatory cytokines is consistent with experiments showing TLR4 was important for inducing signaling in a human monocytic cell line to *A. baumannii*-derived LPS (14).

The mechanisms that regulate the balance of immune response-mediated tissue damage and repair after bacterial infection are beginning to be understood (33). Weight loss during infection is associated with mortality in both human and mouse models of pneumonia (23, 34). Interestingly, despite *A. baumannii* OMV stimulation of TLR4-deficient mice being protected from inflammation, these mice experience more weight loss throughout the infection time course than wild-type mice stimulated with *A. baumannii* OMVs. However, weight was maintained in TLR2-deficient mice stimulated with *A. baumannii* OMVs early after stimulation. This suggests that the weight loss

observed in TLR4-deficient mice was independent of the TLR4-mediated inflammatory responses, and another TLR(s) may play more important roles in metabolism during inflammation. In our models, we did not see significant changes in the recruitment of neutrophils to the lungs between TLR2-deficient and TLR4-deficient mice that were stimulated with *A. baumannii* OMVs. Infection of mice deficient in the expression of TLR2 has delayed wound healing and may be mediated by fibroblasts (35, 36). It is possible that *A. baumannii* OMV-mediated TLR2 activation in cell populations other than macrophages induces tissue repair mechanisms. The mechanisms by which TLRs regulate metabolism are beyond the scope of our investigation and remain an interesting area in which further research should be explored.

Our work described here highlights the effects of bacterium-derived OMVs in mediating inflammatory and tissue pathological responses. Certain strains of *A. baumannii* can disseminate and result in organ infections, sepsis, and death (37–39). It will be interesting to determine if the OMVs contribute to bacterial dissemination and subsequent systemic pathology. The OMVs' trigger of lung inflammation could result in the disruption of lung barrier and thereby contribute to promoting bacterial dissemination.

It has been shown that clinical score and mortality as a result of *A. baumannii* infection correlate with proinflammatory mediators in the lung and histological score more so than bacterial counts (39). It is clear from the findings presented here that bacterium-derived OMVs alone, independent of bacterial growth, can trigger a robust inflammatory response in the lung that is associated with significant tissue pathology. Recent work has shown that the OMVs themselves also have virulence potential due to their phospholipase, hemolytic, and leukotoxic activities (40). Moreover, antibiotic treatments can result in OMV secretion and modulate OMV protein components. Additional research is needed to determine the implications of these OMVs in clinical infection (41).

One possible limitation of our study is that it is not clear how many OMVs are present during the *in vivo A. baumannii* infection. The net amount of OMVs *in vivo* depends not only on the OMV generation by the bacteria but also on the uptake of the bacterial OMVs by the host cells, which makes it difficult to estimate the *in vivo* generation of OMVs by bacteria.

In summary, our investigation has added to the scientific understanding of the mechanisms by which *A. baumannii* OMVs mediate pulmonary inflammation *in vivo*. The pulmonary inflammation was related to neutrophil recruitment and release of several proinflammatory chemokines and cytokines. The inflammation is partly dependent on TLR2 and TLR4, more so on TLR4, suggesting that other PRRs have roles in *A. baumannii* OMV-mediated pulmonary inflammation. The relative importance of OMVs for proinflammatory responses in patients infected with *A. baumannii* remains to be revealed in the future.

MATERIALS AND METHODS

Mice. The Pohang University of Science and Technology and Yale University Animal Care and Use Committee approved all animal experiments that were conducted at the respective institutions.

Isolation of *A. baumannii* OMVs. OMVs were purified from the culture of *A. baumannii* strain KCCM 35453 (ATCC 15150), originally purchased from the Korean Culture Center of Microorganisms (Seoul, South Korea), which was used in other work as previously reported (7, 42, 43), with some modifications. Briefly, *A. baumannii* was cultured in lysogeny broth medium up to an A_{600} of 1.0 at 37°C with gentle shaking (200 rpm). The supernatants were recovered at 6,000 × *g* for 20 min at 4°C and subsequently clarified by a 0.45-μm-pore-sized vacuum filter. The filtrate was concentrated with a QuixStand benchtop system (GE Healthcare Life Sciences, Little Chalfont, UK) equipped with a 100-kDa hollow-fiber membrane (GE Healthcare Life Sciences). Following additional filtration with a 0.22-μm-pore-sized vacuum filter, the concentrate was subjected to ultracentrifugation at 150,000 × *g* for 3 h at 4°C. The pellet was resuspended in 4.8 ml of 50% iodixanol (Sigma-Aldrich, St. Louis, MO, USA)–HEPES-buffered saline (HBS; 20 mM HEPES, 150 mM NaCl, 250 mM sucrose, pH 7.4) to perform three-step density gradient ultracentrifugation at 200,000 × *g* for 2 h at 4°C; the pellet suspension was placed at the bottom of discontinuous density medium, comprised of 3.0 ml of 40% iodixanol–HBS overlaid with 2.5 ml of 10% iodixanol–HBS. Ten fractions with equivalent volumes were retrieved from the top, and the protein concentration for each fraction was measured by Bradford assay (Bio-Rad Laboratories, Hercules, CA, USA). OMVs in the protein-rich fraction were further purified by ultracentrifugation at 150,000 × *g* for 3 h at 4°C.

Characterization of *A. baumannii* OMVs. The size distributions of the purified OMVs were determined by a Zetasizer Nano ZS (Malvern Instrument Ltd., Malvern, UK), equipped with a 633-nm laser line, and analyzed with Zetasizer software (version 6.3.4; Malvern Instruments Ltd.). The results were representative of three independent measurements.

For transmission electron microscopy, the purified OMVs (100 μg/ml in total protein concentration) were absorbed onto glow-discharged carbon-coated copper grids (Electron Microscopy Sciences, Hatfield, PA, USA) for 5 min. Following washing with deionized water, the grids were subjected to negative staining with 2% uranyl acetate (Ted Pella, Redding, CA). Transmission electron micrographs were obtained using a JEM 1011 microscope (JEOL, Tokyo, Japan) at an acceleration voltage of 100 kV. The amount of LPS in *A. baumannii* OMVs was determined using a *Limulus* amebocyte lysate chromogenic endotoxin quantitation kit (Pierce Biotechnology, Rockford, IL). We determined the amount of LPS in *A. baumannii* OMVs, and 1 μg of the OMVs (in total protein amounts) contained 1,269.89 $\pm$ 31.54 endotoxin units.

Production of polyclonal anti-*A. baumannii* OMV antibody. Six-week-old female rabbits (Hyochang Science, Daegu, Republic of Korea) were immunized with *A. baumannii* OMVs (20 μg in total protein amounts) that were emulsified in incomplete Freund's adjuvant (Sigma-Aldrich) for the initial immunization (at day 1) and boosting (at day 14 and day 28). Rabbit sera were retrieved from the rabbit blood on day 31 and were dialyzed against 20 mM sodium phosphate (pH 7.0). The dialyzed sera were adsorbed on a HiTrap protein G column (GE Healthcare Life Sciences) in 20 mM sodium phosphate (pH 7.0), and the bound antibodies were eluted with 100 mM glycine-HCl (pH 2.7). The eluted antibodies were immediately neutralized with 1 M Tris-HCl (pH 9.0), and the neutralized antibodies were dialyzed against PBS overnight at 4°C. Some of the purified antibodies were biotinylated using EZ-Link sulfo-NHS-LC-biotin (Thermo Fisher Scientific, Waltham, MA, USA), the biotinylation was terminated with 1 M ethanolamine (pH 8.0) (Sigma-Aldrich), and free biotin and ethanolamine were removed by dialysis against PBS.

***In vivo* model.** Age- and sex-matched mice were employed for *in vivo* experiments. Wild-type C57BL/6 mice were purchased from Jackson Laboratory (Bar Harbor, ME, USA), and TLR2- and TLR4-deficient mice were the kind gift of Richard Flavell (Yale University). Mice were lightly anesthetized with ketamine-xylazine. Once adequate sedation was achieved, *A. baumannii* OMVs (at 0, 1, 5, or 10 μg in total protein amounts) were instilled via intranasal administration. At 6, 12, 24, or 48 h after introduction of *A. baumannii* OMVs, the mice were euthanized. Bronchoalveolar lavage (BAL) fluid was obtained via intratracheal lung irrigation with two 0.8-ml aliquots of sterile PBS. Cell counting was performed using an AcT 10 automated hematology analyzer (Beckman Coulter, Brea, CA, USA). Differential cell counting of the BAL fluid was performed using a Hemacolor rapid staining kit (Merck Millipore, Billerica, MA) with counting of at least a hundred cells.

***A. baumannii* OMV component detection.** At 6, 12, 24, and 48 h after intranasal administration of *A. baumannii* OMVs, mouse lungs were collected. The lung tissues were homogenized in radioimmunoprecipitation assay (RIPA) buffer (25 mM Tris-HCl, 150 mM NaCl, 2 mM EDTA, 0.5% NP-40 [pH 7.5]) with protease inhibitor cocktails (Sigma-Aldrich). The total protein concentration of the lung lysates was measured with a DC assay (Bio-Rad Laboratories). Unconjugated and biotinylated polyclonal anti-*A. baumannii* OMV antibodies were used to detect *A. baumannii* OMV components from the lung lysates by sandwich enzyme-linked immunosorbent assay (ELISA), whereby unconjugated antibodies were used as capture antibodies and biotinylated antibodies as detection antibodies.

Histological analysis. Anesthetized mice were subjected to whole-body perfusion. The lungs were fixed in 4% paraformaldehyde and then excised for storage overnight at 4°C. Paraffin-embedded lungs were sectioned at 4-μm thickness, deparaffinized with xylene, and rehydrated with an alcohol series. Lung sections were stained with hematoxylin and eosin, and a light microscope was used to acquire images (Olympus, Tokyo, Japan, or Nikon, Tokyo, Japan).

Peritoneal macrophage isolation. The abdomens of wild-type mice and mice deficient in the expression of TLR2, TLR4, or MyD88 were cleaned with 70% ethanol, and then 2 ml of sterile thioglycolate was injected into the peritoneal cavity. Five days after the injection the abdomens were again cleaned with 70% ethanol and the peritoneal cavity was injected with three aliquots of 5 ml ice-cold PBS. The abdomens were gently massaged with the instilled PBS, and then a 22-gauge, half-inch needle with a 10-ml syringe was inserted into the peritoneal cavity. The maximum amount of fluid was removed between each aliquot of ice-cold PBS. The aliquots were collected and the cells were spun at 300 $\times$ *g* at 4°C for 5 min. The cells were resuspended in RPMI 1640 with L-glutamine. The cells were counted using an AcT 10 automated hematology analyzer (Beckman Coulter).

***In vitro* stimulation.** RAW264.7 (a mouse macrophage cell line) cells or peritoneal macrophages were cultured on a 24-well plate (1.0×10^5 cells/well) and treated with various concentrations of *A. baumannii* OMVs (0.01, 0.1, and 1.0 ng/ml in total protein concentrations) in the medium containing 0.5% fetal bovine serum for 12 h. The cell-free conditioned media were collected and stored at -80°C until the cytokine concentrations were determined.

Chemokine and cytokine analysis. The concentrations of chemokines CCL2 and CXCL1 as well as cytokines IL-6, TNF-α, IFN-γ, and IL-1β were measured in cell-free BAL fluid or conditioned medium by a DuoSet ELISA development kit (R&D Systems, Minneapolis, MN, USA) according to the manufacturer's instructions.

Western blot analysis. The lung samples were lysed in RIPA buffer and lysed using a mechanical homogenizer. After incubation on ice for 30 min, the samples were centrifuged to remove the tissue debris. The total protein contents in the supernatants were measured using a bicinchoninic acid (BCA) assay kit (Thermo Scientific). Approximately 40 μg of protein was loaded onto a 4 to 20% gradient gel

(Bio-Rad) after denaturation in Laemmli buffer and run at 120 V for approximately 1 h. Proteins were then transferred to polyvinylidene difluoride membrane using the Trans-Blot system (Bio-Rad). The blots were blocked in 5% nonfat dry milk and then probed with antibodies to p-MAPK, total MAPK (Cell Signaling), and horseradish peroxidase (HRP)-labeled β-actin (Santa Cruz Biotechnologies). For p-MAPK and total MAPK, blots were then incubated with HRP-labeled anti-rabbit secondary antibody (Cell Signaling). The blots were visualized using a Bio-Rad imager after addition of HRP substrate.

qPCR. To perform quantitative PCR (qPCR), a small piece of lung tissue was homogenized in TRIzol reagent and RNA was purified using an RNA isolation kit according to the manufacturer's instructions (Qiagen). Approximately 1 μg of RNA was then reverse transcribed using an iScript cDNA synthesis kit (Bio-Rad). The qPCR was performed using SYBR green (Bio-Rad) with primers for TNF-α, IL-6, IL-1β, IFN-α4, IFN-β, and IFN-γ. The primer sequences are the following: TNF-α forward (F), TAGCCCACGTCGTAGCA AAC; TNF-α reverse (R), ACAAGGTACAACCCATCGGC; IL-6 F, CCGGAGAGGAGACTTCACAG; IL-6 R, TTGCC ATTGCACAACTCTTTT; IL-1β F, CTGAACTCAACTGTGAAATGCCA; IL-1β R, AAAGGTTTGGAAGCAGCCCT; IFN-α4 F, CTTTCCTCATGATCCTGGTAATGAT; IFN-α 4 R, AATCCAAAATCCTTCCTGTCCTTC; IFN-β F, TGTCT GCGAGCCTAGAGACTA; IFN-β R, AGCCGGGAATTTCGTATTGTTAT; IFN-γ F, CCTGTCAGAGGTGTCCCTCG; and IFN-γ R, GGGAGACCTTAGGACAGCTC.

Statistical analysis. Statistical analysis was performed using GraphPad Prism software. The significance of data that followed a normal distribution was determined using a two-tailed Student's *t* test, and the significance of data that did not follow a normal distribution was determined using a nonparametric Mann-Whitney test. For experiments involving more than one comparison, we used one-way analysis of variance followed by a Bonferroni multiple-comparison test. Values were expressed as means $\pm$ standard errors of the means, and statistical significance was defined at a P value of <0.05.

SUPPLEMENTAL MATERIAL

Supplemental material for this article may be found at https://doi.org/10.1128/IAI.00243-19.

SUPPLEMENTAL FILE 1, PDF file, 0.2 MB.

REFERENCES

1. Lin MF, Lan CY. 2014. Antimicrobial resistance in Acinetobacter baumannii: from bench to bedside. World J Clin Cases 2:787–814. https://doi.org/10.12998/wjcc.v2.i12.787.
2. Mayr FB, Yende S, Angus DC. 2014. Epidemiology of severe sepsis. Virulence 5:4–11. https://doi.org/10.4161/viru.27372.
3. Markowicz P, Wolff M, Djedaini K, Cohen Y, Chastre J, Delclaux C, Merrer J, Herman B, Veber B, Fontaine A, Dreyfuss D. 2000. Multicenter prospective study of ventilator-associated pneumonia during acute respiratory distress syndrome. Incidence, prognosis, and risk factors. ARDS Study Group. Am J Respir Crit Care Med 161:1942–1948. https://doi.org/10.1164/ajrccm.161.6.9909122.
4. Kim SB, Min YH, Cheong JW, Kim JS, Kim SJ, Ku NS, Jeong SJ, Han SH, Choi JY, Song YG, Kim JM. 2014. Incidence and risk factors for carbapenem- and multidrug-resistant Acinetobacter baumannii bacteremia in hematopoietic stem cell transplantation recipients. Scand J Infect Dis 46:81–88. https://doi.org/10.3109/00365548.2013.857042.
5. Mendez JA, Soares NC, Mateos J, Gayoso C, Rumbo C, Aranda J, Tomas M, Bou G. 2012. Extracellular proteome of a highly invasive multidrug-resistant clinical strain of Acinetobacter baumannii. J Proteome Res 11:5678–5694. https://doi.org/10.1021/pr300496c.
6. Elhosseiny NM, Amin MA, Yassin AS, Attia AS. 2015. Acinetobacter baumannii universal stress protein A plays a pivotal role in stress response and is essential for pneumonia and sepsis pathogenesis. Int J Med Microbiol 305:114–123. https://doi.org/10.1016/j.ijmm.2014.11.008.
7. Moon DC, Choi CH, Lee JH, Choi CW, Kim HY, Park JS, Kim SI, Lee JC. 2012. Acinetobacter baumannii outer membrane protein A modulates the biogenesis of outer membrane vesicles. J Microbiol 50:155–160. https://doi.org/10.1007/s12275-012-1589-4.
8. Mogensen TH. 2009. Pathogen recognition and inflammatory signaling in innate immune defenses. Clin Microbiol Rev 22:240–273. https://doi.org/10.1128/CMR.00046-08.
9. Mukherjee S, Karmakar S, Babu SP. 2016. TLR2 and TLR4 mediated host immune responses in major infectious diseases: a review. Braz J Infect Dis 20:193–204. https://doi.org/10.1016/j.bjid.2015.10.011.
10. Park BS, Lee JO. 2013. Recognition of lipopolysaccharide pattern by TLR4 complexes. Exp Mol Med 45:e66. https://doi.org/10.1038/emm.2013.97.
11. Cannova J, Breslin SJP, Zhang J. 2015. Toll-like receptor signaling in hematopoietic homeostasis and the pathogenesis of hematologic diseases. Front Med 9:288–303. https://doi.org/10.1007/s11684-015-0412-0.
12. Knapp S, Wieland CW, Florquin S, Pantophlet R, Dijkshoorn L, Tshimbalanga N, Akira S, van der Poll T. 2006. Differential roles of CD14 and Toll-like receptors 4 and 2 in murine Acinetobacter pneumonia. Am J Respir Crit Care Med 173:122–129. https://doi.org/10.1164/rccm.200505-730OC.
13. March C, Regueiro V, Llobet E, Moranta D, Morey P, Garmendia J, Bengoechea JA. 2010. Dissection of host cell signal transduction during Acinetobacter baumannii-triggered inflammatory response. PLoS One 5:e10033. https://doi.org/10.1371/journal.pone.0010033.
14. Erridge C, Moncayo-Nieto OL, Morgan R, Young M, Poxton IR. 2007. Acinetobacter baumannii lipopolysaccharides are potent stimulators of human monocyte activation via Toll-like receptor 4 signalling. J Med Microbiol 56:165–171. https://doi.org/10.1099/jmm.0.46823-0.
15. Quinton LJ, Mizgerd JP. 2015. Dynamics of lung defense in pneumonia: resistance, resilience, and remodeling. Annu Rev Physiol 77:407–430. https://doi.org/10.1146/annurev-physiol-021014-071937.
16. Steiner DJ, Furuya Y, Jordan MB, Metzger DW. 2017. Protective role for macrophages in respiratory Francisella tularensis infection. Infect Immun 85:e00064-17. https://doi.org/10.1128/IAI.00064-17.
17. Wu DD, Pan PH, Liu B, Su XL, Zhang LM, Tan HY, Cao Z, Zhou ZR, Li HT, Li HS, Huang L, Li YY. 2015. Inhibition of alveolar macrophage pyroptosis reduces lipopolysaccharide-induced acute lung injury in mice. Chin Med J 128:2638–2645. https://doi.org/10.4103/0366-6999.166039.
18. Chimen M, Yates CM, McGettrick HM, Ward LS, Harrison MJ, Apta B, Dib LH, Imhof BA, Harrison P, Nash GB, Rainger GE. 2017. Monocyte subsets coregulate inflammatory responses by integrated signaling through TNF and IL-6 at the endothelial cell interface. J Immunol 198:2834–2843. https://doi.org/10.4049/jimmunol.1601281.
19. Mohammadi N, Midiri A, Mancuso G, Patane F, Venza M, Venza I, Passantino A, Galbo R, Teti G, Beninati C, Biondo C. 2016. Neutrophils directly recognize group B streptococci and contribute to interleukin-1beta production during infection. PLoS One 11:e0160249. https://doi.org/10.1371/journal.pone.0160249.
20. Andrews K, Abdelsamed H, Yi AK, Miller MA, Fitzpatrick EA. 2013. TLR2 regulates neutrophil recruitment and cytokine production with minor contributions from TLR9 during hypersensitivity pneumonitis. PLoS One 8:e73143. https://doi.org/10.1371/journal.pone.0073143.
21. Yáñez-Mó M, Siljander PR-M, Andreu Z, Zavec AB, Borràs FE, Buzas EI, Buzas K, Casal E, Cappello F, Carvalho J, Colás E, Cordeiro-da Silva A, Fais S, Falcon-Perez JM, Ghobrial IM, Giebel B, Gimona M, Graner M, Gursel I,

Gursel M, Heegaard NHH, Hendrix A, Kierulf P, Kokubun K, Kosanovic M, Kralj-Iglic V, Krämer-Albers E-M, Laitinen S, Lässer C, Lener T, Ligeti E, Linē A, Lipps G, Llorente A, Lötvall J, Manček-Keber M, Marcilla A, Mittelbrunn M, Nazarenko I, Nolte-'t Hoen ENM, Nyman TA, O'Driscoll L, Olivan M, Oliveira C, Pállinger É, Del Portillo HA, Reventós J, Rigau M, Rohde E, Sammar M, Sánchez-Madrid F, Santarém N, Schallmoser K, Ostenfeld MS, Stoorvogel W, Stukelj R, Van der Grein SG, Vasconcelos MH, Wauben MHM, De Wever O. 2015. Biological properties of extracellular vesicles and their physiological functions. J Extracell Vesicles 4:27066. https://doi.org/10.3402/jev.v4.27066.

22. Park KS, Lee J, Jang SC, Kim SR, Jang MH, Lotvall J, Kim YK, Gho YS. 2013. Pulmonary inflammation induced by bacteria-free outer membrane vesicles from Pseudomonas aeruginosa. Am J Respir Cell Mol Biol 49:637–645. https://doi.org/10.1165/rcmb.2012-0370OC.
23. Marion CR, Wang J, Sharma L, Losier A, Lui W, Andrews N, Elias JA, Kazmierczak BI, Roy CR, Dela Cruz CS. 2016. Chitinase 3-like 1 (Chil1) regulates survival and macrophage-mediated interleukin-1beta and tumor necrosis factor alpha during Pseudomonas aeruginosa pneumonia. Infect Immun 84:2094–2104. https://doi.org/10.1128/IAI.00055-16.
24. Massey S, Yeager LA, Blumentritt CA, Vijayakumar S, Sbrana E, Peterson JW, Brasel T, LeDuc JW, Endsley JJ, Torres AG. 2014. Comparative Burkholderia pseudomallei natural history virulence studies using an aerosol murine model of infection. Sci Rep 4:4305. https://doi.org/10.1038/srep04305.
25. Rabolli V, Lison D, Huaux F. 2016. The complex cascade of cellular events governing inflammasome activation and IL-1beta processing in response to inhaled particles. Part Fibre Toxicol 13:40. https://doi.org/10.1186/s12989-016-0150-8.
26. Awad F, Assrawi E, Jumeau C, Georgin-Lavialle S, Cobret L, Duquesnoy P, Piterboth W, Thomas L, Stankovic-Stojanovic K, Louvrier C, Giurgea I, Grateau G, Amselem S, Karabina SA. 2017. Impact of human monocyte and macrophage polarization on NLR expression and NLRP3 inflammasome activation. PLoS One 12:e0175336. https://doi.org/10.1371/journal.pone.0175336.
27. Dolinay T, Kim YS, Howrylak J, Hunninghake GM, An CH, Fredenburgh L, Massaro AF, Rogers A, Gazourian L, Nakahira K, Haspel JA, Landazury R, Eppanapally S, Christie JD, Meyer NJ, Ware LB, Christiani DC, Ryter SW, Baron RM, Choi AM. 2012. Inflammasome-regulated cytokines are critical mediators of acute lung injury. Am J Respir Crit Care Med 185:1225–1234. https://doi.org/10.1164/rccm.201201-0003OC.
28. Lee EY, Bang JY, Park GW, Choi DS, Kang JS, Kim HJ, Park KS, Lee JO, Kim YK, Kwon KH, Kim KP, Gho YS. 2007. Global proteomic profiling of native outer membrane vesicles derived from Escherichia coli. Proteomics 7:3143–3153. https://doi.org/10.1002/pmic.200700196.
29. Kim DK, Kang B, Kim OY, Choi DS, Lee J, Kim SR, Go G, Yoon YJ, Kim JH, Jang SC, Park KS, Choi EJ, Kim KP, Desiderio DM, Kim YK, Lotvall J, Hwang D, Gho YS. 2013. EVpedia: an integrated database of high-throughput data for systemic analyses of extracellular vesicles. J Extracell Vesicles 2:20384. https://doi.org/10.3402/jev.v2i0.20384.
30. Garcia-Patino MG, Garcia-Contreras R, Licona-Limon P. 2017. The immune response against Acinetobacter baumannii, an emerging pathogen in nosocomial infections. Front Immunol 8:441. https://doi.org/10.3389/fimmu.2017.00441.
31. Jin JS, Kwon SO, Moon DC, Gurung M, Lee JH, Kim SI, Lee JC. 2011. Acinetobacter baumannii secretes cytotoxic outer membrane protein A via outer membrane vesicles. PLoS One 6:e17027. https://doi.org/10.1371/journal.pone.0017027.
32. Li ZT, Zhang RL, Bi XG, Xu L, Fan M, Xie D, Xian Y, Wang Y, Li XJ, Wu ZD, Zhang KX. 2015. Outer membrane vesicles isolated from two clinical Acinetobacter baumannii strains exhibit different toxicity and proteome characteristics. Microb Pathog 81:46–52. https://doi.org/10.1016/j.micpath.2015.03.009.
33. Soares MP, Teixeira L, Moita LF. 2017. Disease tolerance and immunity in host protection against infection. Nat Rev Immunol 17:83–96. https://doi.org/10.1038/nri.2016.136.
34. Piggott DA, Varadhan R, Mehta SH, Brown TT, Li H, Walston JD, Leng SX, Kirk GD. 2015. Frailty, inflammation, and mortality among persons aging with HIV infection and injection drug use. J Gerontol A Biol Sci Med Sci 70:1542–1547. https://doi.org/10.1093/gerona/glv107.
35. Dasu MR, Thangappan RK, Bourgette A, DiPietro LA, Isseroff R, Jialal I. 2010. TLR2 expression and signaling-dependent inflammation impair wound healing in diabetic mice. Lab Investig 90:1628–1636. https://doi.org/10.1038/labinvest.2010.158.
36. Maharjan AS, Pilling D, Gomer RH. 2010. Toll-like receptor 2 agonists inhibit human fibrocyte differentiation. Fibrogenesis Tissue Repair 3:23. https://doi.org/10.1186/1755-1536-3-23.
37. Harris G, Kuo Lee R, Lam CK, Kanzaki G, Patel GB, Xu HH, Chen W. 2013. A mouse model of Acinetobacter baumannii-associated pneumonia using a clinically isolated hypervirulent strain. Antimicrob Agents Chemother 57:3601–3613. https://doi.org/10.1128/AAC.00944-13.
38. Hobson DW, Schuh JC, Zurawski DV, Wang J, Arbabi S, McVean M, Funk KA. 2016. The first cut is the deepest: the history and development of safe treatments for wound healing and tissue repair. Int J Toxicol 35:491–498. https://doi.org/10.1177/1091581816656804.
39. Eveillard M, Soltner C, Kempf M, Saint-André JP, Lemarié C, Randrianarivelo C, Seifert H, Wolff M, Joly-Guillou ML. 2010. The virulence variability of different Acinetobacter baumannii strains in experimental pneumonia. J Infect 60:154–161. https://doi.org/10.1016/j.jinf.2009.09.004.
40. Jha C, Ghosh S, Gautam V, Malhotra P, Ray P. 2017. In vitro study of virulence potential of Acinetobacter baumannii outer membrane vesicles. Microb Pathog 111:218–224. https://doi.org/10.1016/j.micpath.2017.08.048.
41. Yun SH, Park EC, Lee SY, Lee H, Choi CW, Yi YS, Ro HJ, Lee JC, Jun S, Kim HY, Kim GH, Kim SI. 2018. Antibiotic treatment modulates protein components of cytotoxic outer membrane vesicles of multidrug-resistant clinical strain. Clin Proteomics 15:28. https://doi.org/10.1186/s12014-018-9204-2.
42. Kwon SO, Gho YS, Lee JC, Kim SI. 2009. Proteome analysis of outer membrane vesicles from a clinical Acinetobacter baumannii isolate. FEMS Microbiol Lett 297:150–156. https://doi.org/10.1111/j.1574-6968.2009.01669.x.
43. Choi DS, Kim DK, Choi SJ, Lee J, Choi JP, Rho S, Park SH, Kim YK, Hwang D, Gho YS. 2011. Proteomic analysis of outer membrane vesicles derived from Pseudomonas aeruginosa. Proteomics 11:3424–3429. https://doi.org/10.1002/pmic.201000212.